Molecular Devices

# A Unidirectional DNA Walker That Moves Autonomously along a Track**

*Peng Yin, Hao Yan,* Xiaoju G. Daniell, Andrew J. Turberfield,* and John H. Reif**

A major challenge in nanotechnology is to precisely transport a nanoscale object from one location on a nanostructure to another location along a designated path. The successful construction of self-assembled DNA nanostructures provides a solid structural foundation to meet this challenge. DNA, with its immense information-encoding capacity and well-defined Waston–Crick complementarity, has been explored as an excellent building material for nanoconstruction.[1,2] In particular, recent years have seen remarkable success in the construction of both self-assembled nanostructures and individual nanomechanical devices. For example, one- and two-dimensional DNA lattices have been constructed from a rich set of branched DNA molecules.[3–7] These DNA lattices could provide a platform for embedded DNA nanomechanical devices to perform the desired transportation. A diverse group of DNA nanomechanical devices have also been demonstrated. These include DNA nanodevices that execute cycles of motions, such as opening/closing,[8–11] extension/contraction,[12–14] and reversible rotation.[15,16] Such DNA-based nanodevices can be cycled between well-defined states by means of external intervention, for example, by the sequential addition of DNA "fuel strands"[8–10,12–14,16] or by changing the ionic composition of the solution.[11,15] However, these devices are unsuitable for the above challenge for two reasons: First, they demonstrate only local conformation changes, rather than progressive motion. Second, they do not move autonomously. Various schemes of autonomous DNA walker devices based on DNA cleavage and ligation have been explored theoretically but not experimentally;[17] these schemes have been limited to random bidirectional movement. The use of DNA hybridization as an energy source for autonomous molecular motors has also been proposed.[18] The

[*] P. Yin, Prof. H. Yan, X. G. Daniell, Prof. J. H. Reif
Department of Computer Science
Duke University
Durham, NC 27708 (USA)
Fax: (+1) 919-660-6519
E-mail: hy1@cs.duke.edu
reif@cs.duke.edu
Prof. A. J. Turberfield
Department of Physics, Clarendon Laboratory
University of Oxford
Parks Road, Oxford OX1 3PU (UK)
Fax: (+44) 1-865-272
E-mail: a.turberfield@physics.ox.ac.uk

[**] This work was supported by a grant from the NSF (EIA-0218359) to H.Y. and J.H.R., by NSF ITR grants EIA-0086015 and CCR-0326157, and by DARPA/AFSOR Contract F30602-01-2-0561.

Supporting information for this article is available on the WWW under http://www.angewandte.org or from the author.

  DOI: 10.1002/ange.200460522 

construction of a non-autonomous DNA biped walker device[19] and autonomous DNA tweezers[20] have been reported recently. The production of a DNA motor capable of autonomous, unidirectional, progressive linear translational motion is an important next step in the development of DNA-based molecular devices.

Herein we report the design and construction of an autonomous, unidirectional DNA motor that moves along a DNA track. The self-assembled track contains three anchorages at which the walker, a six-nucleotide DNA fragment, can be bound. At each step the walker is ligated to the next anchorage, then cut from the previous one by a restriction endonuclease. Each cut destroys the previous restriction site, and each ligation creates a new site, in such a way that the walker can not move backwards. The motor is powered by the hydrolysis of adenosine triphosphate (ATP), a kinetically inert fuel whose breakdown may be accelerated by many orders of magnitude by protein catalysts.[21] The operation of the motor was verified by tracking the radioactively labeled walker by gel electrophoresis.

The autonomous, unidirectional, along-the-track motion demonstrated by this prototype system represents a novel type of motion for DNA-based nanomechanical devices. The motion of the walker can be extended in principle beyond three anchorages. Embedding a walking device of this kind in a DNA lattice would result in a nanorobotics lattice that could meet the challenge stated above: a nanoscale "walker" that moves autonomously along a designated path over a microscopic structure, thereby serving as a carrier of information and possibly even physical cargo, such as nanoparticles.

The structural design of the device is shown in Figure 1a. (Base sequences for all components are given in the Supporting Information). The track consists of three evenly spaced DNA double-helical "anchorages" (A, B, and C), each tethered to another DNA duplex segment, which forms part of the backbone of the track, by means of a four-nucleotide "hinge". Each anchorage consists of 13 base pairs, with a three-nucleotide single-strand overhang ("sticky end"). Each anchorage is positioned three helical turns (31 or 32 base pairs) away from its nearest neighbors. The duplex segments of the backbone of the track and of the three anchorages are expected to behave like rigid rods, since they are much shorter than the persistence length of duplex DNA (greater than 10 turns).[22,23] In contrast, the four-nucleotide single-strand hinge is expected to be flexible, since the persistence length of the single DNA strand is three nucleotides.[24] A six-nucleotide DNA "walker", labeled * and colored red, moves sequentially along the track from anchorage A to B, then to C.

The device was constructed by mixing stoichiometric amounts of purified DNA oligonucleotides in hybridization buffer (see Experimental Section) and slowly cooling the system from 90 to 37 °C. The solution was then supplemented with T4 ligase, endonuclease PflM I, and endonuclease BstAP I and incubated at 37 °C. The autonomous motion of the walker was initiated by the addition of the energy source ATP.

The recognition sites and restriction patterns of PflM I and BstAP I are shown in Figure 1b. Figure 1c shows the sequence of structural changes that occur during the motion of the walker; on the right-hand side the base sequence at the end of each anchorage at each stage is shown, as well as how these base sequences are transformed by the action of enzymes. The motion of the walker depends on alternate enzymatic ligation and restriction (cleavage). Before the motion starts, the walker, whose position is indicated by *, resides at anchorage A, as shown in panel 0 of Figure 1c. In this state anchorages A* and B have complementary sticky ends, which can hybridize with each other. T4 ligase can then seal the nicks at each end of the newly hybridized section, thus joining the two anchorages covalently (A*+B→A*B); this is an irreversible step that consumes energy provided by the hydrolysis of ATP. The ligation of A*B creates a recognition site for endonuclease PflM I. In process II, PflM I cleaves A*B in such a way that the walker moves to anchorage B: A*B→A+B*. The sticky end of anchorage B* can then hybridize with the complementary sticky end of anchorage C, and the two anchorages are ligated to form B*C in process III. The ligation product B*C contains a recognition site for the second endonuclease BstAP I. In process IV, B*C is cleaved by BstAP I to regenerate anchorage B and create C*. Thus, the walker moves from anchorage B to C to complete the autonomous, programmed motion of the walker.

The motion of the walker is unidirectional: the product of ligation between two neighboring anchorages can only be cleaved such that the walker moves onto the downstream anchorage (A*B and B*C can only be cut such that the walker is left attached to B and C, respectively). Two idling steps are possible: B* can be religated to A and regenerated by restriction by PflM I; similarly, C* can be religated to B and regenerated by BstAP I. However, these idling steps neither reverse nor block the overall unidirectional motion of the walker. Once B* has been ligated to C the walker can never return to A.

The autonomous and unidirectional motion of the walker was verified by using denaturing polyacrylamide gel electrophoresis (PAGE) to track the motion of the walker, which was radioactively labeled. The position reached by the walker in the presence of different combinations of enzymes can be determined by measuring the size of the labeled DNA fragment. Figure 2a is a schematic drawing of the experimental design. The 5′ end of the walker (red) was labeled with $\gamma$-$P^{32}$, represented by a red dot in Figure 2a. Initially, the labeled strand (part of A*) is 52 nucleotides long. The completion of processes I, II, III, and IV can be detected by the appearance of bands corresponding to radioactively labeled DNA fragments of 68, 19, 57, and 41 nucleotides, respectively. The appearance of these bands corresponds to the transfer of the radioactively labeled fragment between the anchorages along the track. The system was incubated at 37 °C in hybridization buffer supplemented with ATP and bovine serum albumin (BSA) in the presence of different combinations of enzymes, which were added to the system simultaneously. Figure 2b is an autoradiograph of a denaturing gel which shows the products formed during each reaction. The system in lane 1 is the control reaction without an enzyme or ATP. In lane 2 T4 ligase and ATP are present: The walker is expected to complete process I to produce a radiolabeled strand of 68 nucleotides, thus corresponding to the formation

  

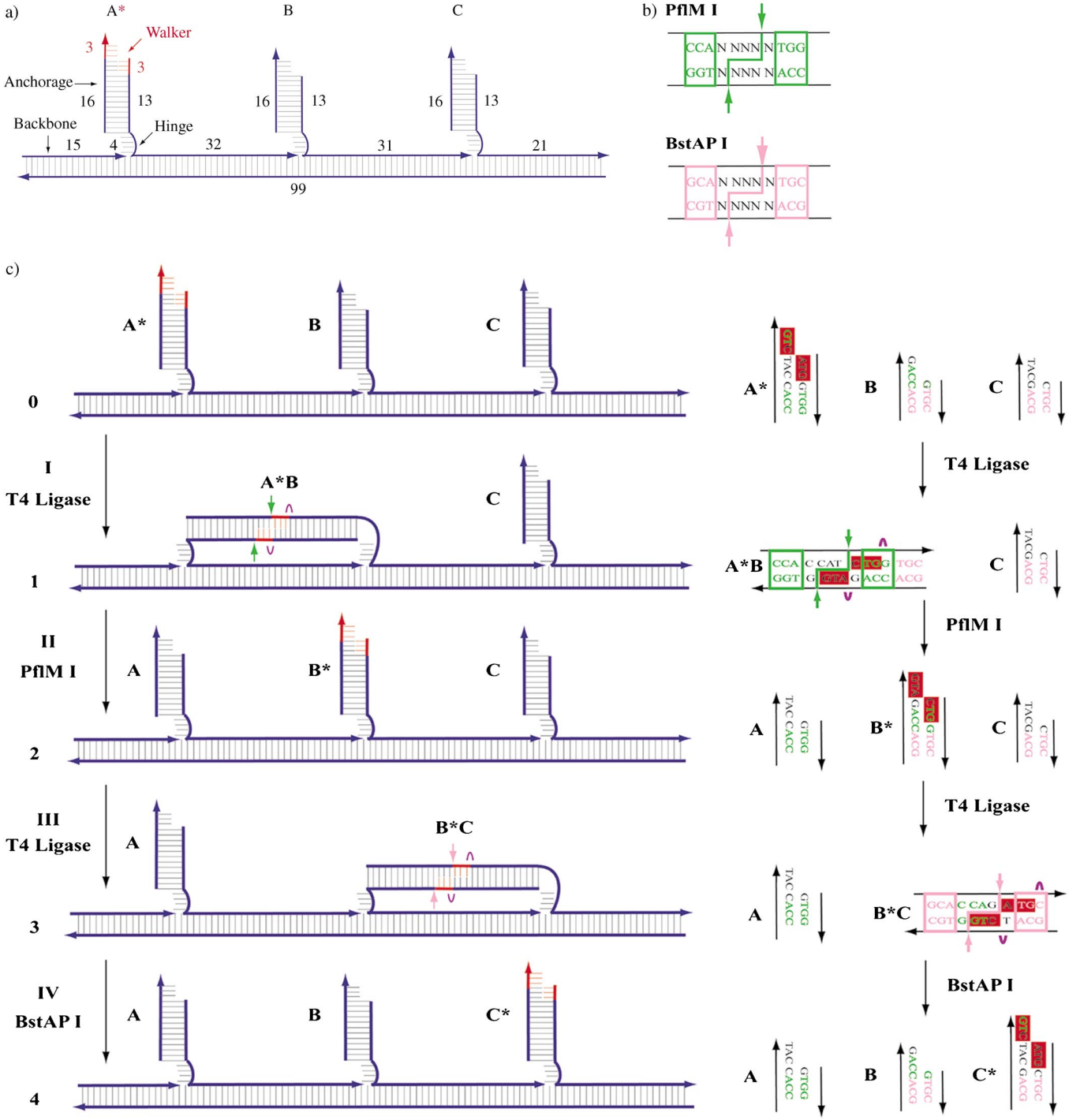


***Figure 1.*** The structural design and operation of the autonomous unidirectional device. a) Structural design: The device contains two parts: the track and the walker. The track consists of three evenly spaced duplex-DNA anchorages, A, B, and C, each linked to the backbone by a hinge: a four-nucleotide flexible single-stranded DNA fragment. The walker is a six-nucleotide DNA fragment (colored red and indicated by *) initially positioned at anchorage A. The numbers give the lengths of DNA fragments in terms of the number of bases. b) Recognition sites and restriction patterns of PflM I and BstAP I: Green (pink) boxes indicate the recognition site of PflM I (BstAP I) and green (pink) arrows indicate their restriction sites. Bases that are important for PflM I (BstAP I) recognition are shown in bold green (pink) fonts. N indicates the position of a base that does not affect recognition. c) Operation of the device: The left-hand scheme shows the sequence of structural changes that occur during the operation of the device; the right-hand scheme describes the accompanying enzymatic reactions and shows how they affect the ends of the anchorages. Panel 0 depicts the device in its initial state. Process I is the ligation of anchorage A* and anchorage B, which have complementary sticky ends; purple curves indicate the ligation sites. Note that the ligation of A* with B creates a PflM I recognition site, which is indicated by green boxes in panel 1; the cuts made by this enzyme are indicated with two green arrows. In process II, the device is cleaved by PflM I, thus transferring the walker to anchorage B (panel 2). The new sticky end of B* is complementary to that of C. In process III, anchorage B* and anchorage C hybridize with each other, and are ligated by T4 ligase to create a recognition site for the endonuclease BstAP I. Purple curves in panel 3 indicate the ligation sites; pink boxes and arrows indicate the BstAP I recognition site and restriction pattern, respectively. In process IV, B*C is cleaved into B and C*, thus transferring the walker to anchorage C and completing the motion of the walker. The final product is shown in panel 4.

  

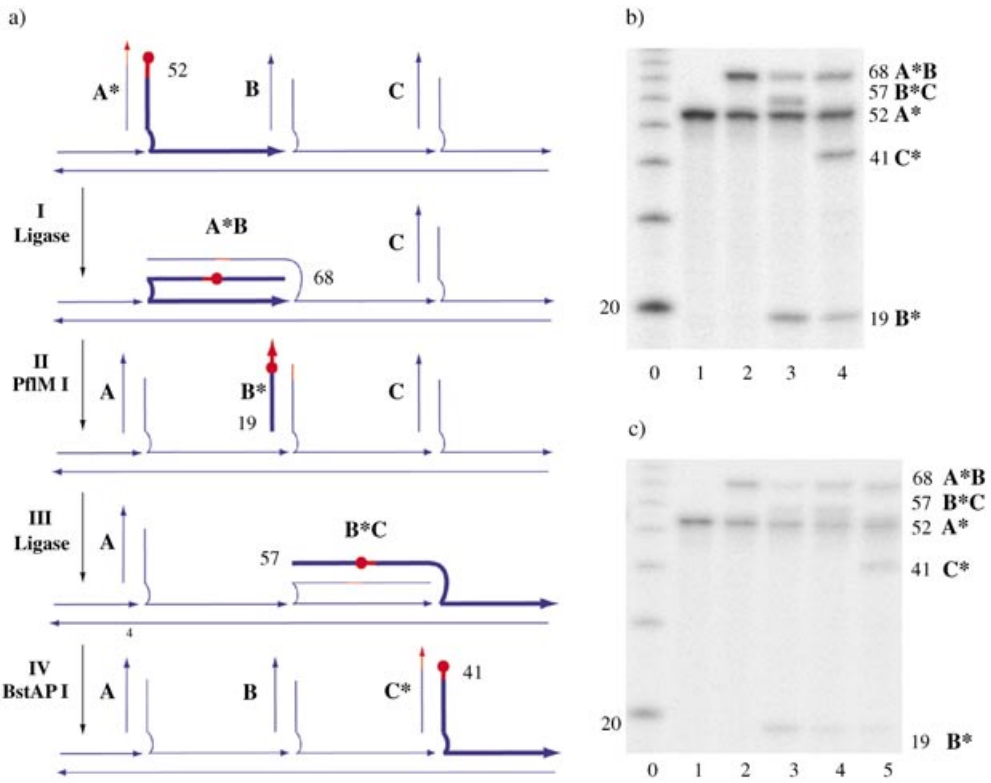


***Figure 2.*** Evidence of the autonomous unidirectional motion of the walker. a) Experimental design: The six-nucleotide walker is colored red. The red dot indicates the radioactive label; at each stage the radioactively labeled strand is illustrated as a thickened line, with its length in terms of the number of bases shown near its 5′ end. b) PAGE analysis of the autonomous motion of the walker. An autoradiograph of a 20% denaturing polyacrylamide gel identifies the position of the radioactively labeled walker. Lane 0: labeled 10-base-pair (bp) DNA ladder marker; lane 1: device with no enzyme (control); lanes 2–4: device with T4 ligase, ATP, and different combinations of the endonucleases PflM I and BstAP I (lane 2: no enzyme; lane 3: with PflM I; lane 4: with BstAP I and PflM I). c) PAGE analysis of the stepwise motion of the walker. Lane 0: labeled 10-bp DNA ladder marker; lane 1: device with no enzyme (control); lanes 2–5: samples corresponding to the stepwise completion of processes I, II, III, and IV in Figure 2a, respectively, as described in the text (lane 2: no enzyme; lane 3: with PflM I; lane 4: no enzyme; lane 5: with BstAP I). Oligonucleotide lengths (in numbers of bases) corresponding to DNA bands are indicated beside the gels.

of A*B. In lane 3 both T4 ligase and endonuclease PflM I are present: The walker is expected to be able to follow the reaction sequence shown in Figure 2a as far as the completion of process III. Upon the completion of process II, A*B is cut to produce A and B*, thus resulting in a labeled strand of 19 nucleotides. Subsequently, B* can be ligated to C to form B*C to give a strand of 57 nucleotides. (These stages in the motion of the walker were also observed in a time-course experiment; see the Supporting Information). In lane 4 all three enzymes are present: The walker is expected to be able to continue autonomously to the completion of process IV in which B*C is cleaved by BstAP I to generate C*, thus producing a labeled strand of 41 nucleotides. The radioactive bands in the gel shown in Figure 2b agree with all the above expectations and hence provide evidence for the designed autonomous, unidirectional motion of the walker.

To further test the operation of the system we forced the device to operate in a stepwise fashion (rather than autonomously) by adding and deactivating the enzymes sequentially. This experiment enabled us to inspect more closely the products formed at the end of each process. The walker was radioactively labeled as described above. Figure 2c is an autoradiograph of a denaturing gel which shows the products after each step. The system was first supplemented with T4 ligase: The appearance of a band corresponding to a 68-nucleotide DNA fragment in lane 2 demonstrates the completion of process I and the formation of A*B. The solution was left at 37 °C for one day to deactivate T4 ligase,[a] then PflM I was added (lane 3). The band of 68 nucleotides, which corresponds to A*B, diminished, whereas a band of 19 nucleotides, which corresponds to B*, appeared, thus confirming the completion of process II. The system was then incubated at 37 °C for two more days to deactivate PflM I,[b] and was again supplemented with T4 ligase and ATP (lane 4). The intensity of the 19-nucleotide band corresponding to B* dramatically decreased, whereas the intensity of the 68-nucleotide band corresponding to A*B increased, and a 57-nucleotide band corresponding to B*C also appeared. This is consistent with our expectation that B* can be ligated to both A and C. The formation of A*B is only an idling step in the motion of the walker. One more day later, after the enzymatic activity of T4 ligase had ceased, the addition of BstAP I resulted in the disappearance of the 57-nucleotide band and the appearance of a 41-nucleotide band, thus indicating the cleavage of B*C to B and C* (lane 5). The intensity of the 68-nucleotide band remained almost unchanged, which confirms that A*B is resistant to the restriction activity of BstAP I. These measurements provide further confirmation that the device operates as designed.

The unidirectional motion of the walker was also tested by the two control experiments depicted in Figure 3. In the first experiment, shown in Figure 3a,b, we intentionally con-

[a] The half-life of T4 ligase at 37 °C is approximately 4 h (New England Biolabs, unpublished observations).
[b] The half-life of PflM I at 37 °C is approximately 16 h (New England Biolabs, unpublished observations).

  

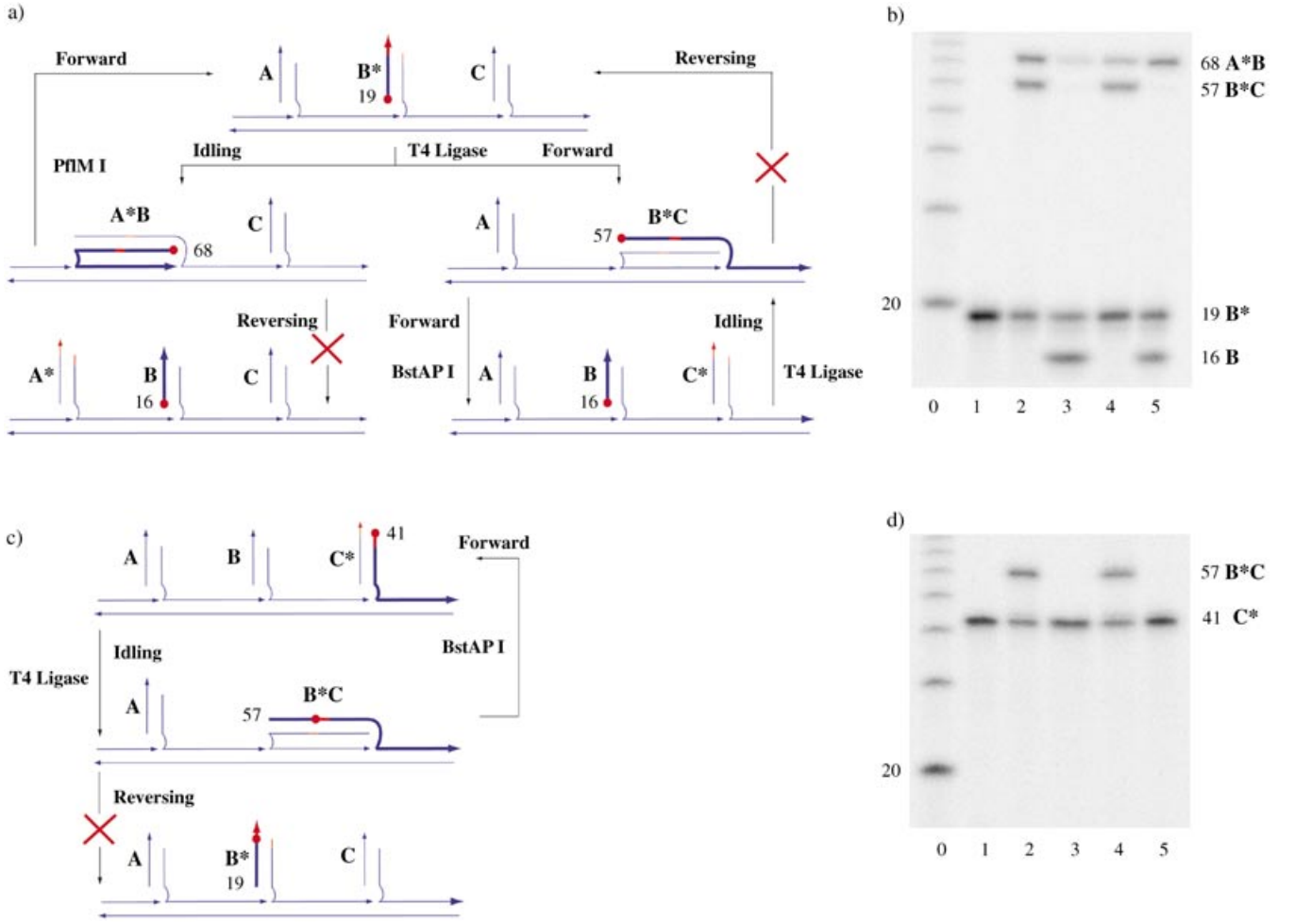


***Figure 3.*** Control experiments. a) and c) show the design of control experiments in which the device is prepared with the walker (colored red) initially attached to anchorages B and C, respectively. Red dots indicate the $\gamma$-$P^{32}$ label; the corresponding labeled strand is shown as a thickened line, with its length in number of bases shown near its 5′ end. A red cross on a broken arrow means that the reaction indicated by that arrow is not expected to happen. b) and d) are autoradiographs of denaturing 20% PAGE gels that show the results of the experiments indicated in parts a) and c), respectively. b),d) Lane 0: labeled 10-bp DNA ladder marker; lane 1: device with no enzyme (control); lanes 2–5: device with T4 ligase, ATP, and different combinations of the endonucleases PflM I and BstAP I (lane 2: no enzyme; lane 3: with BstAP I and PflM I; lane 4: with PflM I; lane 5: with BstAP I). Oligonucleotide lengths (in numbers of bases) corresponding to DNA bands are indicated beside the gels.

structed the device such that the walker initially resides at anchorage B. Figure 3a shows the forward and idling processes that we expect to be allowed, and reverse processes that we expect to be forbidden. The 19-nucleotide strand B* was labeled with $\gamma$-$P^{32}$ at its 5′ end, as indicated by the red dot. Figure 3b shows the products generated upon the addition of different combinations of restriction enzymes and ligase. In the presence of T4 ligase (lane 2 of Figure 3b) the appearance of 68- and 57-nucleotide bands indicate the formation of A*B and B*C, respectively. The addition of BstAP I (lane 5), which is designed to cut B*C into B and C*, leads to a decrease in the intensity of the B*C band and to the generation of the 16-nucleotide fragment B, as expected. The addition of PflM I (lane 4), which is designed to cut A*B into A and B*, leads to a decrease in the intensity of the A*B band, but fragment B is not generated, again as expected. Lane 3 shows the case when all three enzymes are present.

In the second control experiment depicted in Figure 3c, the device was constructed with the walker initially at anchorage C. The 5′ end of the 41-nucleotide strand of anchorage C* was labeled with $\gamma$-$P^{32}$. In the presence of T4 ligase (lane 2 of Figure 3d), the appearance of a 57-nucleotide band indicated the formation of B*C as expected. Subsequent lanes, which correspond to different combinations of restriction enzymes and ligase, show that B*C can be restricted to B and C* by BstAP I as expected, but that no combination of enzymes leads to the reverse step B*C→B*+C (which would have been indicated by a 19-nucleotide labeled band corresponding to B*).

By measuring the intensities of the bands in Figure 2b we estimated the following yields for steps in the operation of the device: A*→A*B, 46%; A*B→B*C, 51%; B*C→C*, 97%. Both imprecise stoichiometry and low ligation/cleavage efficiency could cause low measured yields. Low enzymatic efficiencies might result from the steric constraints imposed

  

by the design of the motor; each substrate is created by hybridization of two anchorages, which are also linked by the backbone of the track. We are currently investigating design improvements, including structural modifications such as an increase in the length of the linkage between each anchorage and the backbone.

As the reactions described herein were carried out in solution, the possibility exists that the anchorages of two individual devices might interact with each other in such a way that the walker of one device might deviate from its designated track and move onto the track of another device. Through a control experiment described in the Supporting Information we have shown that under conditions corresponding to those under which the measurements described above were made, the linkage of two tracks is undetectable.

In summary, we have designed and constructed a nanoscale device in which an autonomous walker moves unidirectionally along a DNA track, driven by the hydrolysis of ATP. The motion of the walker can in principle be extended well beyond the three-anchorage system demonstrated herein.[25] The discovery of new endonucleases with larger nonspecific spacing regions within their recognition sequences could lead to walkers of larger sizes. By encoding information into the walker and the anchorages, it should be possible to develop the device into a powerful autonomous computing device (and hence an "intelligent" robotics device).[26]

## Experimental Section

DNA sequences were designed and optimized with the SEQUIN software[27] and are listed in the Supporting Information. DNA strands were synthesized commercially by Integrated DNA Technology, Inc. (www.idtdna.com) and purified by denaturing gel electrophoresis. The concentrations of DNA strands were determined by measurement of ultraviolet absorption at 260 nm. To assemble the track, the DNA strands were mixed stoichiometrically at 0.3 μM in hybridization buffer and incubated in a heating block from 90 to 37 °C over a period of 3 h. NEB buffer purchased from New England Biolabs (www.neb.com) was used as the hybridization buffer: NEB 3 contains NaCl (100 mM), Tris-HCl (50 mM), $MgCl_2$ (10 mM), and dithiothreitol (1 mM, pH 7.7 at 37 °C). Radioactive labeling: DNA strands were labeled with T4 polynucleotide kinase purchased from Invitrogen Inc. (www.invitrogen.com), by using the standard protocol recommended by the kinase kit. For the ligation experiments and cleavage by the endonucleases, a 30-μL solution containing 1 pmol of the assembled device was supplemented with BSA (100 $\mu g\,mL^{-1}$) and ATP (1 mM). 1 unit of T4 Ligase, 24 units of the endonuclease PflM I, and 5 units of the endonuclease BstAP I were added to the solution, followed by overnight incubation at 37 °C. The endonucleases PflM I and BstAP I were purchased from New England Biolabs (www.neb.com). T4 ligase was purchased from Invitrogen Inc. (www.invitrogen.com). The reaction solution was NEB 3 buffer supplemented with BSA and ATP and containing NaCl (100 mM), Tris-HCl (50 mM), $MgCl_2$ (10 mM), dithiothreitol (1 mM, pH 7.7 at 37 °C), BSA (100 $\mu g\,mL^{-1}$), and ATP (1 mM). The enzymatic reactions were carried out at 37 °C. For denaturing gel electrophoresis, the mixture was heated at 90 °C for 10 min, and applied to denaturing polyacrylamide gel. The positions of the radioactively labeled strands were detected by phosphor imaging. The relative concentrations of DNA present in the bands were measured by using ImageQuant from Molecular Dynamics (www.mdyn.com).

Received: April 30, 2004
Published Online: August 30, 2004

**Keywords:** DNA · molecular devices · nanorobotics · nanostructures · self-assembly

[1] N. C. Seeman, *Nature* **2003**, *421*, 427 – 431.
[2] C. M. Niemeyer, M. Adler, *Angew. Chem.* **2002**, *114*, 3933 – 3937; *Angew. Chem. Int. Ed.* **2002**, *41*, 3779 – 3783.
[3] E. Winfree, F. Liu, L. A. Wenzler, N. C. Seeman, *Nature* **1998**, *394*, 539 – 544.
[4] C. Mao, W. Sun, N. C. Seeman, *J. Am. Chem. Soc.* **1999**, *121*, 5437 – 5443.
[5] T. H. LaBean, H. Yan, J. Kopatsch, F. Liu, E. Winfree, J. H. Reif, N. C. Seeman, *J. Am. Chem. Soc.* **2000**, *122*, 1848 – 1860.
[6] H. Yan, T. H. LaBean, L. Feng, J. H. Reif, *Proc. Natl. Acad. Sci. USA* **2003**, *100*, 8103 – 8108.
[7] H. Yan, S. H. Park, G. Finkelstein, J. H. Reif, T. H. LaBean, *Science* **2003**, *301*, 1882 – 1884.
[8] B. Yurke, A. J. Turberfield, A. P. Mills, Jr., F. C. Simmel, J. L. Neumann, *Nature* **2000**, *406*, 605 – 608.
[9] F. C. Simmel, B. Yurke, *Phys. Rev. E* **2001**, *63*, 041 913.
[10] F. C. Simmel, B. Yurke, *Appl. Phys. Lett.* **2002**, *80*, 883 – 885.
[11] D. Liu, S. Balasubramanian, *Angew. Chem.* **2003**, *115*, 5912 – 5914; *Angew. Chem. Int. Ed.* **2003**, *42*, 5734 – 5736.
[12] L. Feng, S. H. Park, J. H. Reif, H. Yan, *Angew. Chem.* **2003**, *115*, 4478 – 4482; *Angew. Chem. Int. Ed.* **2003**, *42*, 4342 – 4346.
[13] P. Alberti, J.-L. Mergny, *Proc. Natl. Acad. Sci. USA* **2003**, *100*, 1569 – 1573.
[14] J. J. Li, W. Tan, *Nano Lett.* **2002**, *2*, 315 – 318.
[15] C. Mao, W. Sun, Z. Shen, N. C. Seeman, *Nature* **1999**, *397*, 144 – 146.
[16] H. Yan, X. Zhang, Z. Shen, N. C. Seeman, *Nature* **2002**, *415*, 62 – 65.
[17] J. H. Reif, *Lect. Notes Comput. Sci.* **2003**, *2568*, 22 – 37.
[18] A. J. Turberfield, J. C. Mitchell, B. Yurke, A. P. Mills, Jr., M. I. Blakey, F. C. Simmel, *Phys. Rev. Lett.* **2003**, *90*, 118 102.
[19] W. B. Sherman, N. C. Seeman, *Nano Lett.* **2004**, in press.
[20] Y. Chen, M. Wang, C. Mao, *Angew. Chem.* **2004**, *116*, 3638 – 3641; *Angew. Chem. Int. Ed.* **2004**, *43*, 3554 – 3557.
[21] F. H. Westheimer, *Science* **1987**, *235*, 1173 – 1178.
[22] S. B. Smith, L. Finzi, C. Bustamante, *Science* **1992**, *258*, 1122 – 1126.
[23] G. S. Manning, *Biopolymers* **1981**, *20*, 1751 – 1755.
[24] S. B. Smith, Y. Cui, C. Bustamante, *Science* **1996**, *271*, 795 – 799.
[25] "Designs for Autonomous Unidirectional Walking DNA Devices": P. Yin, A. J. Turberfield, J. H. Reif in *Tenth International Meeting on DNA Computing*, **2004**.
[26] "Design for an Autonomous DNA Nanomechanical Device Capable of Universal Computation and Universal Translational Motion": P. Yin, A. J. Turberfield, S. Sahu, J. H. Reif in *Tenth International Meeting on DNA Computing*, **2004**.
[27] N. C. Seeman, *J. Biomol. Struct. Dyn.* **1990**, *8*, 573 – 581.

  